HHS Public Access

Author manuscript

Cancer Discov. Author manuscript; available in PMC 2016 March 01.

Published in final edited form as:

Cancer Discov. 2015 September ; 5(9): 920–931. doi:10.1158/2159-8290.CD-15-0125.

A genome-wide scan identifies variants in *NFIB* associated with metastasis in patients with osteosarcoma

A full list of authors and affiliations appears at the end of the article.

Abstract

Metastasis is the leading cause of death in osteosarcoma patients, the most common pediatric bone malignancy. We conducted a multi-stage genome-wide association study of osteosarcoma metastasis at diagnosis in 935 osteosarcoma patients to determine whether germline genetic variation contributes to risk of metastasis. We identified a SNP, rs7034162, in *NFIB* significantly associated with metastasis in European osteosarcoma cases, as well as in cases of African and Brazilian ancestry (meta-analysis of all cases: $P=1.2\times10^{-9}$, OR 2.43, 95% CI 1.83–3.24). The risk allele was significantly associated with lowered *NFIB* expression, which led to increased osteosarcoma cell migration, proliferation, and colony formation. Additionally, a transposon screen in mice identified a significant proportion of osteosarcomas harboring inactivating insertions in *Nfib*, and had lowered Nfib expression. These data suggest that germline genetic variation at rs7034162 is important in osteosarcoma metastasis, and that *NFIB* is an osteosarcoma metastasis susceptibility gene.

Keywords

osteosarcoma; metastasis; genome-wide association study

Introduction

Metastasis to distant secondary sites is the cause of death for the majority of cancer patients; a defining feature of osteosarcoma is the high rate of metastasis. Osteosarcoma is the most common primary malignant bone tumor with a main incidence peak in adolescence during the pubertal growth spurt, and a second, smaller peak, in the seventh and eighth decade of

*Corresponding Author: Lisa Mirabello, Ph.D., Investigator, Genetics Epidemiology Branch, Division of Cancer Epidemiology and Genetics, National Cancer Institute, 9609 Medical Center Drive, Room 6E422, Bethesda, MD 20850. Tel: 240-276-7258, mirabellol@mail.nih.gov.

[22]These authors contributed equally to this work.

AUTHOR CONTRIBUTIONS

Project design was carried out by L.M., S.A.S., S.J.C. Sample collection, data acquisition, and clinical characterization was performed by J.M.G.F, R.G., C.K., A.M.F., R.T., I.L.A, J.S.W., N.G., L.G.S., D.A.B., N.M., A.P.G., L.S., F.L., M.S., C.H., P.P., K.S., N.K., I.E.I., N.S., S.R.C.T., S.P., M.F.A., D.H., M.L.B., D.M.T., C.D., P.M., S.I.B., M.P.P., N.E.C., M.T., N.R., M.T.L., D.T.S., P.K., D.J.H., N.M., M.K., S.W., R.T., L.H., J.F.F, R.N.H., S.J.C., S.A.S. Genotyping was performed by M.Y., Z.W., J.F.B, B.D.H., A.V., L.B. Statistical analyses were performed by L.M., R.K., N.P. Cell line functional assays were conceived and performed by R.K. Mouse sleeping beauty screen and soft agar colony formation assay was performed by B.S.M., D.L., G.M.O, K.L.B., N.K.W., M.T.W. Immunohistochemical scoring was performed by J.G. The manuscript was written by L.M., R.K, S.A.S., S.J.C., and reviewed by all co-authors.

COMPETING FINANCIAL INTERESTS

The authors declare no competing financial interests.

life (1–3). Epidemiologic data suggests that growth may contribute to osteosarcoma etiology, and several studies have found common genetic variants associated with risk of osteosarcoma (3–6). However, the disease course for osteosarcoma patients is variable, and the pathogenesis and prognostic factors that contribute to this variability remain poorly understood.

Patients presenting with metastatic osteosarcoma have a very poor prognosis with 5-year overall survival rates ranging from 11%–29% (7–10). Approximately 10–25% of osteosarcoma patients have metastases at the time of diagnosis, and up to 90% of these metastasize to the lungs (11–14). Several factors have been inconsistently proposed to be associated with primary metastasis, including older age, low socioeconomic status, larger tumor size, and tumor location (7, 9, 10, 12, 13). However, the largest international collaborative study of osteosarcoma to date found that none of the clinical or demographic factors evaluated were associated with metastasis; they found that the presence of metastasis at diagnosis increased the risk of a subsequent metastasis fivefold (14).

To our knowledge, there have been no studies evaluating the role of genetic variation in osteosarcoma metastasis, and there may be an underlying genetic component contributing to the risk of metastasis. A connection between germline genetic variation and susceptibility to metastasis has been recently reported in other cancers (15–17); however, we are unaware of any studies evaluating the association between germline genetic variation and metastasis in pediatric cancers. Here, we assembled clinical outcome data on 935 osteosarcoma cases from our recent GWAS (5) and four independent replication sets to determine if common germline genetic variation is associated with risk of metastasis at diagnosis of osteosarcoma. We further used *in vitro* studies to functionally characterize a novel metastasis-associated locus.

Results

Variants at 9p24.1 associated with metastasis at diagnosis

The discovery analysis included 541 cases of European ancestry that passed quality control metrics and had data on the presence of confirmed metastases at diagnosis (Supplemental Table 1). Metastatic disease was present in 23% of osteosarcoma patients at diagnosis and was associated with a significantly reduced overall survival (P=1.9×10^{-19}, hazard ratio [HR] 4.3, 95% confidence intervals [CI] 3.13–5.91) (Supplemental Table 2). Age at diagnosis, gender, tumor subtypes, and tumor location were not significantly different in the patients with metastases at diagnosis compared with patients without metastases at diagnosis (Supplemental Table 2).

An adjusted logistic regression model with log-additive effects identified one locus at 9p24.1 associated with metastasis that approached genome-wide significance in our discovery analysis (Supplemental Table 3, Supplemental Figure 1). Specifically, six linked intronic SNPs in the nuclear factor I/B gene (*NFIB*) on chromosome 9p24.1 were significantly associated with an increased risk of metastasis (top SNP rs2890982: P=4.4×10^{-7}, odds ratio [OR] 2.69, 95% CI 1.83–3.94) (Table 1, Figure 1A). Evaluation of

associations with metastasis at diagnosis for the top SNP by inheritance model suggested no departure from the log-additive model (Supplemental Table 4).

We examined variants at 9p24.1 in 85 osteosarcoma cases using targeted genotyping of this region (Replication set 1; Supplemental Table 1). The top 100 SNPs from the discovery set were also evaluated in an additional 141 independent cases with GWAS data (Replication set 2; Supplemental Table 1). A fixed effect meta-analysis was applied to combine the results of each replication set (226 total unique cases) and the discovery set (541 unique cases). In the meta-analysis, the 9p24.1 locus marked by SNP rs2890982 was strongly associated with metastasis at diagnosis ($P=4.9\times10^{-8}$, OR 2.60, 95% CI 1.87–3.62) (Table 1).

To further evaluate this locus, we imputed SNPs across a 1 Mb region centered on the index SNP on 9p24.1. Meta-analyses of the imputed SNPs from both replication sets and the discovery set showed a similar increased risk of metastasis associated with rs7034162 ($P=3.3\times10^{-8}$, OR 2.62, 95% CI 1.86–3.68; $r^2=0.8$ with rs2890982) (Table 1, Figure 1B, Supplemental Table 4). Only the imputed index SNP (rs7034162) additionally showed an association with an increased risk of metastasis in cases of African (N=61) and Brazilian (N=107) ancestry with GWAS data (Supplemental Table 1); in a meta-analysis combining all cases (European discovery/replication, African, and Brazilian ancestry cases; N=935) the rs7034162 association with metastasis gained significance ($=1.2\times10^{-9}$, OR 2.43, 95% CI 1.83–3.24) (Table 1, Figure 1C, Supplemental Table 5).

We additionally evaluated associations for the top SNPs in the European discovery stage cases compared to the European controls from our previous GWAS (N=2703) (5) (minor allele frequencies [MAF] for the controls are shown in Supplemental Table 6). For the top SNP, rs7034162, the minor allele (A) was significantly associated with an increased risk comparing the cases with metastasis to the controls (OR 2.04, 95% CI 1.47–2.82, $P=1.84\times10^{-5}$). Conversely, there was a borderline statistically significant inverse association for the minor allele of rs7034162 comparing the cases without metastasis to the controls (OR 0.77, 95% CI 0.60–0.99, $P=0.039$).

Furthermore, the rs7034162 risk allele (A) was significantly associated with worse overall survival in the European cases (discovery stage; N=522) and in all cases (European discovery, African, and Brazilian ancestry cases; N=684) with survival data, with a per-allele HR of 1.34 (95% CI 1.01–1.77, log-rank $P=0.044$) and 1.45 (95% CI 1.16–1.81, log-rank $P=3.3\times10^{-4}$; Kaplan-Meier survival curve shown in Figure 1D), respectively. When we restricted our survival analyses to only the cases without metastasis at diagnosis, including all cases from the discovery stage, replication 3 and replication 4 (Total N=494), the rs7034162 risk allele (A) was associated with worse overall survival with a per-allele HR of 1.29 (95% CI 0.92–1.80, log-rank $P=0.124$), although not statistically significant.

Both rs2890982 (g.14181653C>T) and rs7034162 (g.14190287 T>A) are located in intron 4 of the *NFIB* gene (Figure 1). For rs2890982, the risk allele (T) frequencies are variable by population ancestry in the 1000 Genomes Project (Phase 1 genotype data from 1094 individuals (18)): African (AFR) 0.70, Asian (ASN) 0.36, American (AMR) 0.21, and European (EUR) 0.14. The risk allele frequencies for rs7034162 (A) show less population

variation: EUR 0.15, AMR 0.18, AFR 0.30, and ASN 0.37; and, an increased risk of metastasis at diagnosis was associated only with the A allele of rs7034162 across all populations studied (Supplemental Table 6).

Sixty-one markers were highly correlated with rs7034162 ($r^2 \geq 0.6$, 1000 Genomes Project CEU data; CEU haplotype block illustrated in Supplemental Figure 2) and were associated with metastasis at diagnosis with $P \leq 1 \times 10^{-5}$. The majority map to potential regulatory elements in the Encyclopedia of DNA Elements (ENCODE) (19) data set (Supplemental Table 6). Notably, the surrogate SNP rs12377502 maps to a DNAseI hypersensitivity region in osteoblast cells, suggesting this SNP may be within an open chromatin region and have regulatory activity in the relevant cells.

Decreased *NFIB* expression is associated with the risk allele of rs7034162

We performed expression quantitative trait locus (eQTL)-based analyses using publically available expression and genotyping data on 17 osteosarcoma cell lines and 29 tumors (20). We evaluated whether top-ranking SNPs were associated with expression of *NFIB* or other neighboring protein-encoding genes. The risk allele (A) of rs7034162 was significantly associated with a decrease in *NFIB* expression in osteosarcoma cell lines (N=17, P=0.0059) and osteosarcoma tumors (N=29, P=0.0211) (Figure 2, Supplemental Figure 3). There was no association between rs7034162 genotypes and expression of other nearby protein-encoding genes (*FREM1, ZDHHC21, MPDZ*; Figure 2, Supplemental Figure 4).

NFIB expression levels are associated with migration and growth of osteosarcoma cells

The ability of tumor cells to invade and migrate is an important marker of metastatic potential. Therefore, to evaluate the possible involvement of NFIB in osteosarcoma metastatic potential we analyzed the invasion and migration capacity of three human osteosarcoma cell lines (U2OS, HOS, OSA) with different expression levels of *NFIB*. U2OS and HOS cells carry the homozygous non-risk allele (rs7034162: TT) whereas OSA cells carry the homozygous risk allele (rs7034162: AA). U2OS and HOS had significantly higher *NFIB* expression levels and higher NFIB protein levels than OSA cells (Figure 3A, Supplemental Figures 3 and 5A). A matrigel transwell invasion and migration assay demonstrated that the invasion and migration rates were inversely correlated with *NFIB* expression levels in the osteosarcoma cell lines (Figure 3AB). Small interfering RNA (siRNA) molecules against NFIB were used to deplete NFIB; all three osteosarcoma cell lines showed reduced NFIB mRNA and protein levels compared with control (si-NEG) treated cells (Figure 3A, Supplemental Figure 5B). After knockdown of NFIB there was an increase of invasion and migration in all three osteosarcoma cells compared with the control (Figure 3B). U2OS and HOS cells, with high endogenous NFIB expression, had a statistically significant increase in invasion and migration after NFIB knockdown (P=0.009 and 0.015, respectively). In the OSA cell line, with low endogenous NFIB expression, there was a small non-significant increase in invasion and migration after NFIB suppression (P=0.151; Figure 3AB). These findings were confirmed in wound healing cell migration assays and filamentous actin staining assays; there was increased migration of osteosarcoma cells treated with siRNA against NFIB compared with the control (Figure 4ABC). Staining

for filamentous actin showed increased podia formation in all three osteosarcoma cell lines after NFIB suppression (shown for U2OS in Figure 4C), typical of migrating cells.

We blindly replicated our findings using a soft agar colony formation assay in HOS, OSA, and U2OS cells. Over-expression of *NFIB* resulted in a significant reduction in colony formation in HOS ($P<0.0001$) and OSA ($P<0.0001$) cells (Figure 4D). The U2OS cells did not show a significant change in colony formation with *NFIB* over-expression. This was expected since *NFIB* expression is already high in U2OS (Figure 3A, Supplemental Figure 3 and 5A). Additionally, over-expression of *NFIB* resulted in a significant reduction of wound healing in HOS and OSA cells (data not shown).

NFIB is a transcription factor that regulates insulin-like growth factor binding protein 5 (IGFBP5) expression in human osteoblasts, and IGFBP5 has been shown to inhibit tumor growth and metastasis of human osteosarcoma cells (21, 22). Therefore, we evaluated if there was a relationship between *NFIB* and *IGFBP5* expression levels in osteosarcoma cell lines and tumors. We found a statistically significant direct correlation between *NFIB* and *IGFBP5* expression levels ($P=1.17\times10^{-5}$; Supplemental Figure 6). The AA risk allele of rs7034162 was significantly associated with lower *IGFBP5* and *NFIB* expression in osteosarcoma cell lines and tumors (Supplemental Figure 3). The U2OS and HOS cells, both carrying the homozygous non-risk allele (rs7034162: TT), had higher *NFIB* and *IGFBP5* expression levels than the OSA cells (carrying the homozygous risk allele, rs7034162: AA; Supplemental Figures 3 and 7). In addition, *NFIB* siRNA suppression led to the down-regulation of *IGFBP5* in HOS and U2OS cells (Supplemental Figure 7).

Mice with primary osteosarcomas and metastases harbor inactivating transposon insertions in *Nfib*

A connection between *Nfib* and osteosarcoma was also identified in a *sleeping beauty* (*SB*) transposon mutagenesis system in mice (23). A significant proportion of primary osteosarcomas and metastases harbored inactivating transposon insertions in *Nfib* in an analysis of insertions from all chromosomes, including mice on a *Trp53* deficient and wild type background (TAPDANCE Analysis: $P=2.06\times10^{-6}$) (Figure 5A). We evaluated tumor tissues from these mice and found a reduced expression of both *Nfib* ($P=0.087$) and *Igfbp5* ($P=0.048$) in tumors with inactivating transposon insertions compared with tumors lacking insertions in *Nfib* (Figure 5B and 5C). We used immunohistochemical (IHC) staining for NFIB in sections of mouse tumor and adjacent bone to further evaluate tissue-specific changes in NFIB expression. There was a significantly reduced labeling intensity in the osteosarcoma cells with an *Nfib* insertion compared with the adjacent normal osteoblasts ($P=0.0018$; Figure 5D and 5E). There was no NFIB labeling of any osteoclast cells. These mouse data confirm our human cell line findings and further suggest that a decreased expression of *NFIB*, leading to down-regulation of *IGFBP5*, is important for metastatic ability.

Discussion

This first multi-stage GWAS of osteosarcoma metastasis identified a common SNP, rs7034162, in *NFIB* at 9p24.1 associated with metastasis at diagnosis of osteosarcoma. We

replicated the strong association identified in 541 European patients in an additional 394 patients from four case studies, including patients of European, African and Brazilian ancestry. Our data showed that the risk SNP was associated with a decrease in *NFIB* expression, and importantly there was no association with expression of other nearby protein-encoding genes. Therefore, we focused on characterizing the role of NFIB in osteosarcoma metastatic potential.

NFIB is a member of the NFI gene family, which are site-specific DNA-binding proteins, also known as CAAT box transcription factors, they function in both viral DNA replication and in the regulation of genes expressed in almost every organ and tissue (24). NFIB's transcriptional activation or repression of specific gene promoters varies depending on cell type and gene promoter and it modulates the expression of over 100 diverse tissue-specific genes (24). NFIB gene rearrangements and fusions with either HMGA2 or MYB have been reported in lipoma, salivary gland, breast, and head and neck tumors (25–28). Changes in NFIB expression have been associated with specific microRNAs, and NFIB has been reported as a tumor suppressor in some cancers and an oncogene in other cancers (29–33). This implication in both the inhibition and promotion of tumor development and progression in different cancers corroborates the diverse and distinct roles of NFIB in specific tissues and cancer sites. *NFIB* has not been previously implicated in osteosarcoma etiology or osteosarcoma metastasis. Here, we have shown that lowered NFIB leads to increased osteosarcoma cell line migration, proliferation, and colony formation, which suggests its involvement in osteosarcoma metastasis. The mouse *sleeping beauty* transposon mutagenesis screen independently identified *Nfib* with close to genome-wide significance to be a tumor suppressor gene (23), and we further showed that osteosarcomas in mice with *Nfib* insertions had significantly reduced NFIB compared with the adjacent normal osteoblasts.

Since NFIB had previously been shown to directly regulate IGFBP5 expression in human osteoblasts (34), the relevant cell type, we hypothesized that the association of NFIB with osteosarcoma metastases may be mediated through IGFBP5. Interestingly, IGFBP5 has been previously shown to inhibit tumor growth and metastasis of human osteosarcoma cells (21, 22), growth of mouse osteosarcoma cells (35) and migration of human breast cancer cells (36). IGFBP5 is the most abundant IGFBP stored in bone, and it has been shown to regulate osteoblast proliferation and differentiation (37, 38). Thus, NFIB may modulate osteoblast proliferation and differentiation through the modulation of IGFBP5 expression. IGFBP5 can also both inhibit and enhance insulin-like growth factors (IGF), the critical regulators of bone metabolism (38). The IGF-1/IGF-1R axis is important for metastasis and migration, and has been associated with osteosarcoma risk and survival (20, 39–46). We found a direct correlation between *NFIB* and *IGFBP5* expression in osteosarcoma cell lines and tumors, and the rs7034162 risk allele of *NFIB* was also associated with reduced *IGFBP5* expression. We hypothesize that the *NFIB* risk allele leads to lowered expression of *NFIB* and *NFIB*-mediated lower expression of *IGFPB5*, which results in less IGFBP5-mediated inhibition of IGF-1 (47). This may then lead to an IGF-1/IGF-1R axis mediated increase in proliferation, survival, and metastasis of osteosarcoma cells (Supplemental Figure 8).

Metastatic osteosarcoma at diagnosis signifies a poor prognosis, and in our study 23% of patients had metastasis at diagnosis. There are few factors that have been consistently associated with risk of metastasis (14). We have identified a connection between germline genetics and osteosarcoma metastasis at diagnosis, and further showed that the risk SNP likely has a role in osteosarcoma metastasis through an effect on NFIB expression levels. Our data suggests that germline genetic variation at rs7034162 in the *NFIB* gene contributes to susceptibility to metastasis at diagnosis in osteosarcoma patients.

Methods

Study populations

A summary of the participating studies is given in Supplemental Table 1. 541 osteosarcoma cases of European ancestry were included in the discovery set from our previous GWAS, as described (5). 333 unique osteosarcoma cases for replication of the discovery set findings were from the Genetic Epidemiology of Osteosarcoma study (COG AEPI05N2), the registry component of the Children's Oncology Group (COG), through the University of Minnesota as previously described (6); International Sarcoma Kindred Study, Melbourne, VIC (Australia); Therapeutically Applicable Research to Generate Effective Treatments (TARGET) dataset (48); and, from the Instituto de Oncologia Pediátrica GRAACC/UNIFESP and Universidade Federal de Sao Paulo (Brazil). TARGET data was only used for the analysis of the *NFIB* gene region. Cases from COG AEPI05N2 were restricted to those of European ancestry as in the discovery set (5). Cases of African ancestry were identified in four studies in the discovery set (Supplemental Table 1) in our previous GWAS ancestry evaluation using a STRUCTURE analysis and principal component analysis (5).

Patients were diagnosed in the individual hospitals and were prospectively followed up as part of their osteosarcoma treatment. Study centers provided data on patient and clinical variables that were harmonized between the studies, including age at diagnosis, gender, survival, relapse, follow-up, tumor subtype, tumor location, and the presence of histologically confirmed metastatic or non-metastatic disease at diagnosis. All tumors were histologically confirmed. Not all patients had all variable data. In this study we focused on the presence or absence of metastatic disease at diagnosis and did not exclude cases that experienced a later relapse. Participating subjects provided informed consent; studies were conducted in accordance with the Declaration of Helsinki and approved by local Institutional Review Boards.

Genotyping

Germline genomic DNA was extracted from either blood or buccal cells drawn from osteosarcoma case series using standard methods. Genotyping of all cases with GWAS data was conducted using the Illumina OmniExpress SNP microarray. Quality control filtering was performed as previously described (5). We included autosomal SNPs with a MAF of ≥5% in the discovery stage, SNPs with a ≥90% completion rate, and SNPs with no evidence of deviation from Hardy-Weinberg proportion ($P>1\times10^{-7}$). SNPs were excluded if they had abnormal heterozygosity values of <20% or >31%; expected duplicates; and abnormal X-chromosome heterozygosity. There were 29 duplicated cases with concordance rates of

99.96%. Genotypes for all subject pairs were also computed for close relationships (1–2nd degree) using GLU qc.ibds module (49) with an IBD0 threshold of 0.70; no first-degree relatives were identified in the cases scanned. 447,040 SNPs passed quality control metrics for the 541 discovery set cases for final analysis. Only cases of >80% European ancestry were included in the discovery GWAS and the replication COG AEPI05N2 analysis based on STRUCTURE analysis (50) and PCA (51) as previously determined (5). PCA (52) results for individuals in the discovery stage are show in Supplemental Figure 9; there were no significant differences between populations (P >0.1).

The top *NFIB* SNPs associated with metastasis at diagnosis from the discovery set were genotyped using Taqman assays in the International Sarcoma Kindred Study cases, and data from TARGET for osteosarcoma cases was used to examine *NFIB* SNPs (Replication set 1). The top 100 SNPs associated with metastasis at diagnosis were chosen for follow-up in the COG AEPI05N2 cases (Replication set 2) and in cases of African and Brazilian ancestry with GWAS data.

We validated the top imputed SNP, rs7034162, to confirm the imputed genotype using TaqMan assays in 89 cases with GWAS data from the discovery stage (16% of the total 541 cases). TaqMan® assay (Life Technologies) validation and SNP genotyping was performed at the Cancer Genomics Research Facility. The imputation genotype error rate was 1.12% (1 case had the wrong genotype).

Genomic annotation

For all imputed and genotyped SNPs with a P value of less than 1×10^{-5} (N=75) in the *NFIB* locus genomic annotation of SNP markers was conducted using the Encyclopedia of DNA Elements (ENCODE) (19) tool HaploReg (53), RegulomeDB (54) and LDlink (55).

eQTL analysis

We performed expression quantitative trait locus (eQTL)-based analyses using publically available genotype and expression data from 17 osteosarcoma cell lines (GSE36004) and 29 tumors (GSE33383) (20). U2OS, HOS and SJAS-1 (OSA) osteosarcoma cell lines were included as part of the 17 osteosarcoma cell lines with data and are highlighted in Supplemental Figures 3 and 4.

Cell lines

The human osteosarcoma cell lines U2OS, HOS and SJAS-1 (OSA) were obtained from the American Type Culture Collection (ATCC) for our *in vitro* studies (March 2014). Cell lines were tested for authentication (February 2015) with a panel of short tandem repeats (STR) using the Identifiler kit (Life Technologies) and compared with the ATCC STR Profile Databases. Osteosarcoma cells were maintained at 37°C in a humidified atmosphere with 5% CO_2 in RPMI 1640 (Cellgro) supplemented with 10% fetal calf serum (FCS) (Gibco, Life Techonolgies).

PB/SB-CAG-GOI-GFP-PGK-PURO based transposon over expression vectors were generated using the LR Clonase Gateway cloning system (Invitrogen) with cDNAs in Entry

vectors with the previously described PB/SB-CAG-DEST-GFP-PGK-PURO, following manufacturer's instructions (56). Nfib was purchased from Open Biosystems in Gateway ready pENTR221 vector. Nfib and Luciferase over expression cell lines were generated by electroporation using 2 μg PB7 transposase and 2 μg transposon plasmid with the NEON transfection system (Invitrogen), following manufacturer's protocol. After two days cells were selected with 1 μg/mL puromycin to obtain stable cell lines.

RNA interference

A mix of three small interfering RNA (siRNA) molecules against NFIB and a negative control siRNA (ON-TARGETplus™, D-001810-01-20, Thermo Scientific) were purchased from Dharmacon. Subconfluent osteosarcoma cells were transfected in 6-well plates using Lipofectamine® RNAiMAX Transfection Reagent according to the manufacturer's instructions (Life Technologies). Efficacy of the transfection protocol was tested using siGLO™ (D-001630-02-20) according to the manufacturer's instructions (Thermo Scientific). NFIB sequences used were 1) AGGAUACUCUGAAGAACUAUU, 2) GCAAAAGACCCAAAACUAUUU and 3) ACUAGAAGAAGCCUGAAAUU.

RNA isolation and Quantitative real-time PCR for NFIB and IGFBP5

Total RNA was isolated using the RNeasy Mini Kit according to the manufacturer's instructions (Qiagen). cDNA was synthesized from total RNA using the High-Capacity cDNA Reverse Transcription Kit, as described by the manufacturer's protocol (Applied Biosystems, Life Technologies). Quantitative real-time PCR was performed using TaqMan® Gene Expression Master Mix (Life Technologies). The expression of NFIB (Hs01029175_m1) and IGFBP5 (Hs00181213_m1) were normalized to the level of HPRT1 (4326321E) in the same sample, resulting in a ΔCt from which the $2^{-\Delta Ct}$ value was derived and compared with control treated U2OS cells. Results of at least three experiments in triplicate are expressed as mean ± SD.

Cell invasion/migration by transwell matrigel assay

Subconfluent osteosarcoma cells were infected with the indicated siRNAs or controls. 48 hours post-infection, osteosarcoma cells were seeded in RPMI onto the basement membrane matrix (Corning® BioCoat™ Matrigel® Invasion Chambers). The transwell was placed in a 24-well plate that contained 500 μl RPMI 1640 with 10% fetal calf serum as chemo attractant. After 24 hours, the non-invading cells and Matrigel matrix were gently removed with a cotton swab. Invasive cells located on the lower side of the chamber were stained with crystal violet, air-dried and photographed. To quantify cell invasion/migration, the inserts were treated with 200 μl methanol and the absorbance measured in triplicate at 560 nm using the GloMax®-Multi Detection System (Promega). Results of at least three experiments in triplicate are expressed as mean ± SD.

Wound healing cell migration assay

Subconfluent osteosarcoma cells were infected with the indicated siRNAs or controls. Wounds were made on the monolayers using a pipette tip 48 hours post-infection. Bright field images were taken at time 0 and 16, 24 and/or 30 hours (h). After the final image (at

16, 24 or 30h), the plates were washed, cells fixed with methanol and stained with Crystal Violet (C008 Hardy Diagnostics).

Filamentous actin staining

Cells were seeded on coverslips and treated for 48 hours with siRNA as indicated. 6 hours after wounds were made, cells were fixed with 4% paraformaldehyde in PBS for 10 minutes and blocked with 0.1% Triton X-100 and 1% BSA in PBS for 20 minutes. This was followed by incubation with Alexa Fluor® 488 Phalloidin (Life Technologies) in 0.1% Triton X-100 and 1% BSA in PBS for 20 minutes to stain filamentous actin. Finally cells were mounted with ProLong® Diamond Antifade Mountant with DAPI (Life Technologies). The LSM 700 confocal laser scanning microscope (Zeiss) was used for analysis.

Soft agar colony formation assay

Cells (1×10^4) were seeded into soft agar in single wells of six well plates and allowed to incubate for 2–3 weeks. The resultant colonies were then stained with 0.5% crystal violet in buffered formalin for 1 hour. Each well was divided into 4 quadrants and photographed. Colonies were quantified using ImageJ software using a standard colony quantification macro.

Osteosarcoma Sleeping Beauty (SB) Screen

The results of the complete SB screen have been previously published (23). Briefly, mice were generated to target *SB* mutagenesis only in osteoblast cells in wild type or *Trp53* deficient mice. Genes found to be significantly mutated by transposon mutagenesis were then identified. gCIS analysis of T2/Onc insertion sites was performed using gene-centric software, as previously described (57).

RNA was extracted from SB mutagenized tumors using the RNA mini-prep kit (Invitrogen) and reverse transcribed into cDNA using the Superscript III reverse transcriptase kit (Invitrogen), following manufacturer's instructions. Eleven primary tumors with insertions in *Nfib* and 11 primary tumors without insertions in *Nfib* were analyzed. Quantitative RT-PCR was performed using FastStart Universal SYBR Green Master (Rox) mix (Roche) using an Eppendorf Realplex2 Mastercycler EP Gradient S. Primer sequences were as follows, Nfib For-TTCCCCAAGATTGAGCACTT, Nfib Rev-GGATAGCTTGCGTCGGAAA, Igfbp5 For-GTACCTGCCCAACTGTGAC, Igfbp5 Rev-GCTTCATTCCGTACTTGTCCA and normalized to Gapdh, For-GTGTTCCTACCCCCAATGTGT and Rev-GAGACAACCTGGTCCTCAGTGT.

Western blot and Immunohistochemistry staining

Tissues were fixed in 10% buffered formalin and embedded in paraffin blocks. Sections were cut at 5-μm thickness, and rehydrated through a series of graded ethanols. Slides underwent antigen retrieval by boiling for 30 minutes in antigen unmasking solution (Vector Laboratories Inc. Burlington, CA). Endogenous peroxidases were quenched with 3% hydrogen peroxide solution for 20 minutes. For antibody staining, 10% goat serum in 1X PBS-T was used for blocking and antibody incubations. Primary *NFIB* antibody was used at 1:250 (HPA003956; Sigma-Aldrich St. Louis, MO). Following a series of washes, slides

were incubated with biotinylated goat anti-rabbit secondary antibody (1:250; Vector Laboratories Inc. Burlington, CA). Slides were washed, incubated with the vectastain ABC kit (Vector Laboratories Inc. Burlington, CA) for 30 minutes at room temperature, washed again, and stained using peroxidase substrate kit DAB (Vector Laboratories Inc. Burlington, CA). Finally slides were counterstained with hematoxylin, dehydrated, cleared with xylene and mounted with permount (Fisher Scientific Waltham, MA). Immunoblot analysis was performed on whole cell lysates harvested using RIPA buffer (Sigma-Aldrich St. Louis, MO) supplemented with phosphatase inhibitors and protease inhibitors (Sigma-Aldrich St. Louis, MO). Lysates were separated by SDS-PAGE, transferred to a PVDF membrane (Invitrogen Waltham, MA), incubated in 5% BSA in TBST to block nonspecific binding and probed with appropriate antibodies. Proteins were detected on a LI-COR Odyssey Fc instrument using a chemiluminescent HRP substrate (Advansta). *NFIB* antibody used for IHC above was also utilized for immunoblot analysis.

Staining intensity within 16 tumors and adjacent, normal osteoblasts (internal positive control) was assessed by the semi-quantitative H-Score (58), which was determined by summing the products of the percent of cells with weak (1 × %), moderate (2 × %), and strong (3 × %) nuclear staining, with a maximum possible score of 300.

Statistical analyses

Cases with confirmed metastasis at diagnosis were compared with cases without metastasis at diagnosis. In the discovery and replication stages, risk of metastasis at diagnosis was estimated using logistic regression to calculate the odds ratio (OR) and 95% confidence intervals (CIs) per copy of the minor allele assuming a multiplicative (log-additive) genetic model with 1 degree of freedom. Logistic regression models were adjusted for study center; age and gender were not significantly associated with metastasis, and thus, were removed from the model. Since there were no significant eigenvectors from the PCA of osteosarcoma cases (P >0.1), they were not included in the model. The estimated inflation factor, λ, of the test statistic for the discovery set was 0.9107 (Supplemental Figure 10). Logistic regression models for the evaluation of SNP associations comparing the European discovery stage cases with the European controls from our previous GWAS (5) were adjusted for gender and the two significant Eigenvectors from the PCA of cases and controls. We had 91.9% power to detect an OR of 2.60 with 122 cases with metastasis and 419 cases without metastasis at an alpha of 0.05 and allele frequency of 10%.

An inverse-variance fixed-effect meta-analysis was applied to combine the results of the discovery set and replication sets. Between-stages heterogeneity was quantified with I^2 (59). We did not observe significant heterogeneity for the top reported SNPs: rs2890982, EUR meta-analysis of discovery and replication sets: I^2 = 0%, P_{het} = 0.39; rs7034162, all ancestry meta-analysis of discovery and replication sets: I^2 = 17.9%, P_{het} = 0.30.

We imputed additional SNPs within 1 Mb on either side of the implicated SNPs using IMPUTE2 software and the reference data from both the 1000 Genomes project (March 2012 release; [18]) and the DCEG Imputation Reference Set version 1 (60). SNPTEST was used to analyze the posterior SNP dosages from IMPUTE2, adjusting for study center, as described above (61).

A time-to-event analysis for overall survival was assessed in the osteosarcoma cases with these data using Cox proportional hazards regression to estimate hazard ratios and 95% confidence intervals adjusted for study center, ancestry, gender and age. Not all cases had follow-up and survival data; only 522 European ancestry cases included in the discovery stage, 57 African ancestry cases in the replication 3, and 105 Brazilian ancestry cases in the replication 4. Overall survival time was estimated as the time from the date of diagnosis until the date of death or the last known alive date; patients were censored at the last date to be alive or if lost to follow-up. Kaplan-Meier survival curves were created and *P*-values estimated with a Mantel-Cox log-rank test.

Supplementary Material

Refer to Web version on PubMed Central for supplementary material.

Authors

Lisa Mirabello[1,22,*], Roelof Koster[1,22], Branden S. Moriarity[2,3,4,5], Logan G. Spector[2], Paul S. Meltzer[6], Joy Gary[7], Mitchell J. Machiela[1], Nathan Pankratz[8], Orestis A. Panagiotou[1], David Largaespada[2,3,4,5], Zhaoming Wang[9], Julie M. Gastier-Foster[10], Richard Gorlick[11], Chand Khanna[6], Silvia Regina Caminada de Toledo[12], Antonio S. Petrilli[12], Ana Patiño-Garcia[13], Luis Sierrasesúmaga[13], Fernando Lecanda[13], Irene L. Andrulis[14], Jay S. Wunder[14], Nalan Gokgoz[14], Massimo Serra[15], Claudia Hattinger[15], Piero Picci[15], Katia Scotlandi[15], Adrienne M. Flanagan[16,17], Roberto Tirabosco[17], Maria Fernanda Amary[17], Dina Halai[17], Mandy L. Ballinger[18], David M. Thomas[19], Sean Davis[6], Donald A. Barkauskas[20], Neyssa Marina[21], Lee Helman[6], George M. Otto[3], Kelsie L. Becklin[4], Natalie K. Wolf[4], Madison T. Weg[3], Margaret Tucker[1], Sholom Wacholder[1], Joseph F. Fraumeni Jr[1], Neil E. Caporaso[1], Joseph F. Boland[9], Belynda D. Hicks[9], Aurelie Vogt[9], Laurie Burdett[9], Meredith Yeager[9], Robert N. Hoover[1], Stephen J. Chanock[1], and Sharon A. Savage[1]

Affiliations

[1]Division of Cancer Epidemiology and Genetics, National Cancer Institute, National Institutes of Health, Bethesda, MD, USA

[2]Department of Pediatrics, University of Minnesota Minneapolis, MN, 55455, USA

[3]Masonic Cancer Center, University of Minnesota Minneapolis, MN, 55455, USA

[4]Department of Genetics, Cell Biology, and Development, University of Minnesota Minneapolis, MN, 55455, USA

[5]Center for Genome Engineering, University of Minnesota Minneapolis, MN, 55455, USA

[6]Center for Cancer Research, National Cancer Institute, National Institutes of Health, Bethesda, MD 20892, USA

[7]Laboratory of Cancer Biology and Genetics, NCI, NIH, Bethesda, MD, USA, and College of Veterinary Medicine, Michigan State University, East Lansing, MI, USA

[8]Department of Laboratory Medicine and Pathology, University of Minnesota Minneapolis, MN, 55455, USA

[9]Cancer Genomics Research Laboratory, Leidos Biomedical Research, Frederick National Laboratory for Cancer Research, Frederick, MD, USA

[10]Nationwide Children's Hospital, and The Ohio State University Department of Pathology and Pediatrics, 700 Children's Dr., C0988A, Columbus, OH 43205, USA

[11]Albert Einstein College of Medicine, The Children's Hospital at Montefiore, 3415 Bainbridge Avenue, Rosenthal Room 300, Bronx, New York 10467, USA

[12]Pediatric Oncology Institute, GRAACC/UNIFESP, Rua Botucatu, 743 8º andar Laboratorio de Genética, CEP 04023-061 São Paulo SP Brazil

[13]Department Of Pediatrics, University Clinic of Navarra, Universidad de Navarra, Pío XII 36, 31080 Pamplona, Spain

[14]University of Toronto, Litwin Centre for Cancer Genetics, Lunenfeld Tanenbaum Research Institute, Mt Sinai Hospital, 600 University Ave., Toronto, Ontario, Canada, M5G 1X5

[15]Laboratory of Experimental Oncology, Orthopaedic Rizzoli Institute, Bologna, Italy

[16]UCL Cancer Institute, Huntley Street, London WC1E 6BT, UK

[17]Royal National Orthopaedic Hospital NHS Trust, Stanmore, Middlesex HA7 4LP, UK

[18]Peter MacCallum Cancer Centre, St Andrew's Place, East Melbourne, Victoria, Australia

[19]The Kinghorn Cancer Centre, Garvan Institute of Medical Research, Darlinghurst, NSW, Australia

[20]Department of Preventive Medicine, Keck School of Medicine of the University of Southern California, Los Angeles, CA, 90032

[21]Stanford University & Lucile Packard Children's Hospital, 1000 Welch Rd, Suite 300 Palo Alto, CA 94304, USA

Acknowledgments

We thank Dr. Giovanna Maganoli for tissue banking, Dr. Marilù Fanelli for DNA isolation, and Dr. Cristina Ferrari for updating of clinicopathologic data at the Orthopaedic Rizzoli Institute. We thank Anthony Griffin and Diana Marsilio for data collection and Teresa Selander and the Biospecimen Repository staff at Mount Sinai Hospital, Toronto. We acknowledge the advice of Francisco Real at the Spanish National Cancer Research Centre, CNIO. We also thank Francine Tesser Gamba at the Pediatric Oncology Institute, GRAACC-UNIFESP, São Paulo SP Brazil.

Funding Support: This study was funded by the intramural research program of the Division of Cancer Epidemiology and Genetics, National Cancer Institute, National Institutes of Health. This work was supported by the Bone Cancer Research Trust UK to A.M.F. This work was supported by grants to L.G.S. from the National Institutes of Health U01CA122371, and from The Zach Sobiech Osteosarcoma Fund of Children's Cancer Research

Fund. Research is supported by the Chair's Grant U10 CA98543 and Human Specimen Banking Grant U24 CA114766 of the Children's Oncology Group from the National Cancer Institute, National Institutes of Health, Bethesda, MD, USA. Additional support for research is provided by a grant from the WWWW (QuadW) Foundation, Inc. to the Children's Oncology Group. This work was supported by grants to I.L.A. and J.S.W. from the Ontario Research Fund, and Canadian Foundation for Innovation. This study was also supported by biobank grants from the Regione Emilia-Romagna, by the infrastructure and personnel of the Royal National Orthopaedic Hospital Musculoskeletal Research Programme and Biobank. Support was also provided to A.M.F. (UCL) by the National Institute for Health Research UCLH Biomedical Research Centre, and UCL Experimental Cancer Centre, funding from PI13/01476, FIS, ISCIII and La Fundación Bancaria "La Caixa", Fundación Caja Navarra to AP-G and L.S., and AECC project to F.L. The International Sarcoma Kindred Study was supported by the Rainbows for Kate Foundation, the Liddy Shriver Sarcoma Initiative, the Victorian Cancer Agency, the Australian National Health and Medical Research Council (APP1004017) and Cancer Australia (APP1067094).

Abbreviation list

GWAS	genome-wide association study
SNP	single nucleotide polymorphism
OR	odds ratio
HR	hazard ratio
CI	confidence intervals
AFR	African
ASN	Asian
AMR	American
EUR	European
LD	linkage disequilibrium
siRNA	small interfering RNA
eQTL	expression quantitative trait locus
ENCODE	Encyclopedia of DNA Elements
IHC	immunohistochemical

References

1. Mirabello L, Troisi R, Savage S. Osteosarcoma incidence and survival rates from 1973 to 2004: Data from the Surveillance, Epidemiology, and End Results Program. Cancer. 2009; 115:1531–43. [PubMed: 19197972]
2. Mirabello L, Troisi R, Savage S. International osteosarcoma incidence patterns in children and adolescents, middle ages and elderly persons. Int J Cancer. 2009; 125:229–34. [PubMed: 19330840]
3. Savage S, Mirabello L. Using epidemiology and genomics to understand osteosarcoma etiology. Sarcoma. 2011; 2011:548151. [PubMed: 21437228]
4. Mirabello L, Pfeiffer R, Murphy G, Daw N, Patiño-Garcia A, Troisi R, et al. Height at diagnosis and birth-weight as risk factors for osteosarcoma. Cancer Causes Control. 2011; 22:899–908. [PubMed: 21465145]
5. Savage SA, Mirabello L, Wang Z, Gastier-Foster JM, Gorlick R, Khanna C, et al. Genome-wide association study identifies two susceptibility loci for osteosarcoma. Nat Genet. 2013; 45:799–803. [PubMed: 23727862]

6. Musselman JR, Bergemann TL, Ross JA, Sklar C, Silverstein KA, Langer EK, et al. Case-parent analysis of variation in pubertal hormone genes and pediatric osteosarcoma: a Children's Oncology Group (COG) study. Int J Mol Epidemiol Genet. 2012; 3:286–93. [PubMed: 23205180]
7. Meyers PA, Heller G, Healey JH, Huvos A, Applewhite A, Sun M, et al. Osteogenic sarcoma with clinically detectable metastasis at initial presentation. Journal of Clinical Oncology. 1993; 11:449–53. [PubMed: 8445419]
8. Tsuchiya H, Kanazawa Y, Abdel-Wanis ME, Asada N, Abe S, Isu K, et al. Effect of Timing of Pulmonary Metastases Identification on Prognosis of Patients With Osteosarcoma: The Japanese Musculoskeletal Oncology Group Study. Journal of Clinical Oncology. 2002; 20:3470–7. [PubMed: 12177108]
9. Kager L, Zoubek A, Pötschger U, Kastner U, Flege S, Kempf-Bielack B, et al. Primary Metastatic Osteosarcoma: Presentation and Outcome of Patients Treated on Neoadjuvant Cooperative Osteosarcoma Study Group Protocols. Journal of Clinical Oncology. 2003; 21:2011–8. [PubMed: 12743156]
10. Mialou V, Philip T, Kalifa C, Perol D, Gentet J-C, Marec-Berard P, et al. Metastatic osteosarcoma at diagnosis. Cancer. 2005; 104:1100–9. [PubMed: 16015627]
11. Gorlick R, Khanna C. Osteosarcoma. Journal of bone and mineral research. 2010; 25:683–91. [PubMed: 20205169]
12. Bielack SS, Kempf-Bielack B, Delling G, Exner GU, Flege S, Helmke K, et al. Prognostic Factors in High-Grade Osteosarcoma of the Extremities or Trunk: An Analysis of 1,702 Patients Treated on Neoadjuvant Cooperative Osteosarcoma Study Group Protocols. Journal of Clinical Oncology. 2002; 20:776–90. [PubMed: 11821461]
13. Miller BJ, Cram P, Lynch CF, Buckwalter JA. Risk Factors for Metastatic Disease at Presentation with Osteosarcoma. J Bone Joint Surg Am. 2013; 95:e89. [PubMed: 23824394]
14. Pakos EE, Nearchou AD, Grimer RJ, Koumoullis HD, Abudu A, Bramer JAM, et al. Prognostic factors and outcomes for osteosarcoma: An international collaboration. European Journal of Cancer. 2009; 45:2367–75. [PubMed: 19349163]
15. Leongamornlert D, Saunders E, Dadaev T, Tymrakiewicz M, Goh C, Jugurnauth-Little S, et al. Frequent germline deleterious mutations in DNA repair genes in familial prostate cancer cases are associated with advanced disease. Br J Cancer. 2014; 110:1663–72. [PubMed: 24556621]
16. Castro E, Goh C, Olmos D, Saunders E, Leongamornlert D, Tymrakiewicz M, et al. Germline BRCA Mutations Are Associated With Higher Risk of Nodal Involvement, Distant Metastasis, and Poor Survival Outcomes in Prostate Cancer. Journal of Clinical Oncology. 2013; 31:1748–57. [PubMed: 23569316]
17. Bertucci F, Lagarde A, Ferrari A, Finetti P, Charafe-Jauffret E, Van Laere S, et al. 8q24 Cancer Risk Allele Associated with Major Metastatic Risk in Inflammatory Breast Cancer. PLoS ONE. 2012; 7:e37943. [PubMed: 22666420]
18. 1000 Genomes Project Consortium. A map of human genome variation from population-scale sequencing. Nature. 2010; 467:1061–73. [PubMed: 20981092]
19. The ENCODE Project Consortium. An integrated encyclopedia of DNA elements in the human genome. Nature. 2012; 489:57–74. [PubMed: 22955616]
20. Kuijjer ML, Peterse EF, van den Akker BE, Briaire-de Bruijn IH, Serra M, Meza-Zepeda LA, et al. IR/IGF1R signaling as potential target for treatment of high-grade osteosarcoma. BMC Cancer. 2013; 13:245. [PubMed: 23688189]
21. Luther GA, Lamplot J, Chen X, Rames R, Wagner ER, Liu X, et al. IGFBP5 domains exert distinct inhibitory effects on the tumorigenicity and metastasis of human osteosarcoma. Cancer Lett. 2013; 336:222–30. [PubMed: 23665505]
22. Su Y, Wagner ER, Luo Q, Huang J, Chen L, He BC, et al. Insulin-like growth factor binding protein 5 suppresses tumor growth and metastasis of human osteosarcoma. Oncogene. 2011; 30:3907–17. [PubMed: 21460855]
23. Moriarity BS, Otto GM, Rahrmann EP, Rathe SK, Wolf NK, Weg MT, et al. A Sleeping Beauty forward genetic screen identifies new genes and pathways driving osteosarcoma development and metastasis. Nat Genet. 2015; 47:615–24. [PubMed: 25961939]

24. Gronostajski RM. Roles of the NFI/CTF gene family in transcription and development. Gene. 2000; 249:31–45. [PubMed: 10831836]
25. Italiano A, Ebran N, Attias R, Chevallier A, Monticelli I, Mainguené C, et al. NFIB rearrangement in superficial, retroperitoneal, and colonic lipomas with aberrations involving chromosome band 9p22. Genes, Chromosomes and Cancer. 2008; 47:971–7. [PubMed: 18663748]
26. Pierron A, Fernandez C, Saada E, Keslair F, Hery G, Zattara H, et al. HMGA2–NFIB fusion in a pediatric intramuscular lipoma: a novel case of NFIB alteration in a large deep-seated adipocytic tumor. Cancer Genetics and Cytogenetics. 2009; 195:66–70. [PubMed: 19837271]
27. Persson M, Andrén Y, Mark J, Horlings HM, Persson F, Stenman G. Recurrent fusion of MYB and NFIB transcription factor genes in carcinomas of the breast and head and neck. Proceedings of the National Academy of Sciences. 2009; 106:18740–4.
28. Mitani Y, Li J, Rao PH, Zhao Y-J, Bell D, Lippman SM, et al. Comprehensive Analysis of the MYB-NFIB Gene Fusion in Salivary Adenoid Cystic Carcinoma: Incidence, Variability, and Clinicopathologic Significance. Clinical Cancer Research. 2010; 16:4722–31. [PubMed: 20702610]
29. Moon H-G, Hwang K-T, Kim J-A, Kim HS, Lee M-J, Jung E-M, et al. NFIB is a potential target for estrogen receptor-negative breast cancers. Molecular Oncology. 2011; 5:538–44. [PubMed: 21925980]
30. Zhou M, Zhou L, Zheng L, Guo L, Wang Y, Liu H, et al. miR-365 Promotes Cutaneous Squamous Cell Carcinoma (CSCC) through Targeting Nuclear Factor I/B (NFIB). PLoS ONE. 2014; 9:e100620. [PubMed: 24949940]
31. Mosakhani N, Pazzaglia L, Benassi M, Borze I, Quattrini I, Picci P, et al. MicroRNA expression profiles in metastatic and non-metastatic giant cell tumor of bone. Histol Histopathol. 2013; 28:671–8. [PubMed: 23172052]
32. Fujita S, Ito T, Mizutani T, Minoguchi S, Yamamichi N, Sakurai K, et al. miR-21 Gene Expression Triggered by AP-1 Is Sustained through a Double-Negative Feedback Mechanism. Journal of Molecular Biology. 2008; 378:492–504. [PubMed: 18384814]
33. Dooley AL, Winslow MM, Chiang DY, Banerji S, Stransky N, Dayton TL, et al. Nuclear factor I/B is an oncogene in small cell lung cancer. Genes & Development. 2011; 25:1470–5. [PubMed: 21764851]
34. Pérez-Casellas LA, Wang X, Howard KD, Rehage MW, Strong DD, Linkhart TA. Nuclear Factor I transcription factors regulate IGF binding protein 5 gene transcription in human osteoblasts. Biochimica et Biophysica Acta (BBA) – Gene Regulatory Mechanisms. 2009; 1789:78–87. [PubMed: 18809517]
35. Schneider MR, Zhou R, Hoeflich A, Krebs O, Schmidt J, Mohan S, et al. Insulin-like growth factor-binding protein-5 inhibits growth and induces differentiation of mouse osteosarcoma cells. Biochem Biophys Res Commun. 2001; 288:435–42. [PubMed: 11606061]
36. Sureshbabu A, Okajima H, Yamanaka D, Tonner E, Shastri S, Maycock J, et al. IGFBP5 induces cell adhesion, increases cell survival and inhibits cell migration in MCF-7 human breast cancer cells. J Cell Sci. 2012; 125:1693–705. [PubMed: 22328518]
37. Schneider MR, Wolf E, Hoeflich A, Lahm H. IGF-binding protein-5: flexible player in the IGF system and effector on its own. J Endocrinol. 2002; 172:423–40. [PubMed: 11874691]
38. Conover C. Insulin-like growth factor-binding proteins and bone metabolism. Am J Physiol Endocrinol Metab. 2008; 294:E10–4. [PubMed: 18003717]
39. Kappel CC, Velez-Yanguas MC, Hirschfeld S, Helman LJ. Human osteosarcoma cell lines are dependent on insulin-like growth factor I for in vitro growth. Cancer Res. 1994; 54:2803–7. [PubMed: 8168113]
40. Herzlieb N, Gallaher BW, Berthold A, Hille R, Kiess W. Insulin-like growth factor-I inhibits the progression of human U-2 OS osteosarcoma cells towards programmed cell death through interaction with the IGF-I receptor. Cell Mol Biol (Noisy-le-grand). 2000; 46:71–7. [PubMed: 10726973]
41. Hong SH, Briggs J, Newman R, Hoffman K, Mendoza A, LeRoith D, et al. Murine osteosarcoma primary tumour growth and metastatic progression is maintained after marked suppression of serum insulin-like growth factor I. Int J Cancer. 2009; 124:2042–9. [PubMed: 19132750]

42. Burrow S, Andrulis IL, Pollak M, Bell RS. Expression of insulin-like growth factor receptor, IGF-1, and IGF-2 in primary and metastatic osteosarcoma. J Surg Oncol. 1998; 69:21–7. [PubMed: 9762887]
43. Jentzsch T, Robl B, Husmann M, Bode-Lesniewska B, Fuchs B. Worse prognosis of osteosarcoma patients expressing IGF-1 on a tissue microarray. Anticancer Res. 2014; 34:3881–9. [PubMed: 25075009]
44. Chen KT, Hour MJ, Tsai SC, Chung JG, Kuo SC, Lu CC, et al. The novel synthesized 6-fluoro-(3-fluorophenyl)-4-(3-methoxyanilino)quinazoline (LJJ-10) compound exhibits anti-metastatic effects in human osteosarcoma U-2 OS cells through targeting insulin-like growth factor-I receptor. Int J Oncol. 2011; 39:611–9. [PubMed: 21667022]
45. Mansky PJ, Liewehr DJ, Steinberg SM, Chrousos GP, Avila NA, Long L, et al. Treatment of metastatic osteosarcoma with the somatostatin analog OncoLar: significant reduction of insulin-like growth factor-1 serum levels. J Pediatr Hematol Oncol. 2002; 24:440–6. [PubMed: 12218590]
46. Wang YH, Han XD, Qiu Y, Xiong J, Yu Y, Wang B, et al. Increased expression of insulin-like growth factor-1 receptor is correlated with tumor metastasis and prognosis in patients with osteosarcoma. J Surg Oncol. 2012; 105:235–43. [PubMed: 21866554]
47. Conover CA, Kiefer MC. Regulation and biological effect of endogenous insulin-like growth factor binding protein-5 in human osteoblastic cells. J Clin Endocrinol Metab. 1993; 76:1153–9. [PubMed: 7684391]
48. TARGET. Therapeutically Applicable Research to Generate Effective Treatments. Available from: http://ocg.cancer.gov/programs/target
49. Jacobs, K. glu-genetics. Available from: http://code.google.com/p/glu-genetics/
50. Stepulak A, Luksch H, Gebhardt C, Uckermann O, Marzahn J, Sifringer M, et al. Expression of glutamate receptor subunits in human cancers. Histochemistry and cell biology. 2009; 132:435–45. [PubMed: 19526364]
51. Luksch H, Uckermann O, Stepulak A, Hendruschk S, Marzahn J, Bastian S, et al. Silencing of selected glutamate receptor subunits modulates cancer growth. Anticancer Res. 2011; 31:3181–92. [PubMed: 21965725]
52. Patterson N, Price AL, Reich D. Population structure and eigenanalysis. PLoS Genet. 2006; 2:e190. [PubMed: 17194218]
53. Ward LD, Kellis M. HaploReg: a resource for exploring chromatin states, conservation, and regulatory motif alterations within sets of genetically linked variants. Nucleic Acids Research. 2012; 40:D930–D4. [PubMed: 22064851]
54. Boyle AP, Hong EL, Hariharan M, Cheng Y, Schaub MA, Kasowski M, et al. Annotation of functional variation in personal genomes using RegulomeDB. Genome research. 2012; 22:1790–7. [PubMed: 22955989]
55. Machiela, M.; Chanock, S. LDlink: A web-based application for exploring population-specific haplotype structure and linking correlated alleles of potentially functional variants. 2015. Available from: http://analysistools.nci.nih.gov/LDlink/
56. Rahrmann EP, Watson AL, Keng VW, Choi K, Moriarity BS, Beckmann DA, et al. Forward genetic screen for malignant peripheral nerve sheath tumor formation identifies new genes and pathways driving tumorigenesis. Nat Genet. 2013; 45:756–66. [PubMed: 23685747]
57. Brett BT, Berquam-Vrieze KE, Nannapaneni K, Huang J, Scheetz TE, Dupuy AJ. Novel molecular and computational methods improve the accuracy of insertion site analysis in Sleeping Beauty-induced tumors. PLoS ONE. 2011; 6:e24668. [PubMed: 21931803]
58. Goulding H, Pinder S, Cannon P, Pearson D, Nicholson R, Snead D, et al. A new immunohistochemical antibody for the assessment of estrogen receptor status on routine formalin-fixed tissue samples. Hum Pathol. 1995; 26:291–4. [PubMed: 7890280]
59. Higgins JP, Thompson SG, Deeks JJ, Altman DG. Measuring inconsistency in meta-analyses. BMJ. 2003; 327:557–60. [PubMed: 12958120]
60. Wang Z, Jacobs KB, Yeager M, Hutchinson A, Sampson J, Chatterjee N, et al. Improved imputation of common and uncommon SNPs with a new reference set. Nat Genet. 2012; 44:6–7. [PubMed: 22200770]

61. Marchini J, Howie B, Myers S, McVean G, Donnelly P. A new multipoint method for genome-wide association studies by imputation of genotypes. Nat Genet. 2007; 39:906–13. [PubMed: 17572673]

Statement of significance

Metastasis at diagnosis in osteosarcoma is the leading cause of death in these patients. Here we show data that is supportive for the *NFIB* locus as associated with metastatic potential in osteosarcoma.

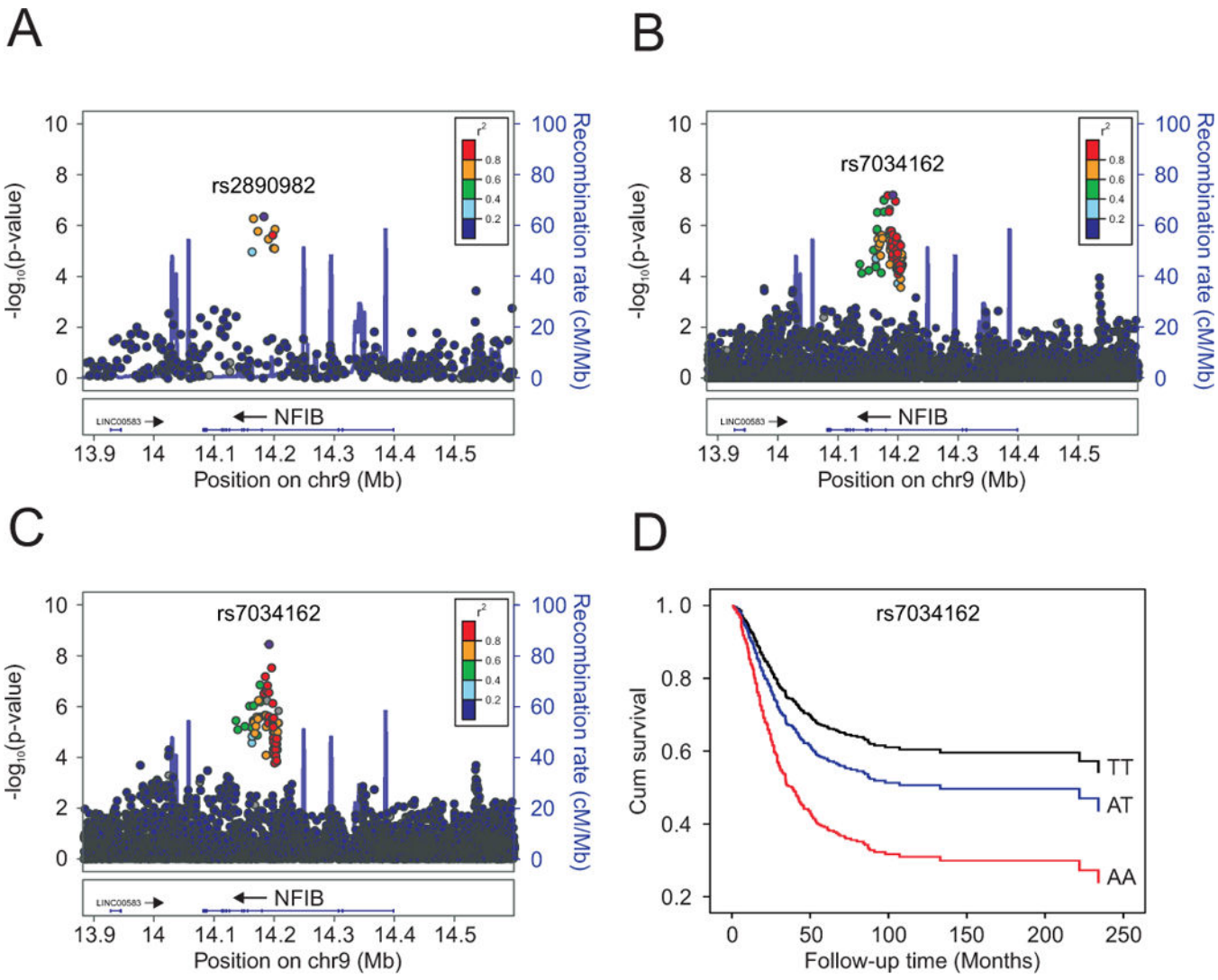

Figure 1. Regional plots of the discovery and combined association results, recombination hotspots and linkage disequilibrium (LD) for the 9p24.1:14,081,842-14,398,982 osteosarcoma metastasis susceptibility locus

Y-axes represent the statistical significance (−log10 transformed *P* values) of SNP association results from a trend test (left) and the recombination rate (right). SNPs are color-coded based on pairwise linkage disequilibrium (r^2) with the most statistically significant SNP. The most statistically significant SNP is labeled and shown in purple. Allelic *P* values generated by SNPTEST using score method (two-sided). Physical locations of the SNPs are based on NCBI human genome build 36, and gene annotation was based on the NCBI RefSeq genes from the UCSC Genome Browser. (**A.**) European discovery set, (**B.**) meta-analyzed European discovery and replication sets (imputed), (**C.**) meta-analyzed European discovery/replication sets, plus African and Brazilian ancestry cases (imputed). (**D**.) Kaplan-Meier curve of cumulative (cum) survival for osteosarcoma patients by rs7034162 genotype.

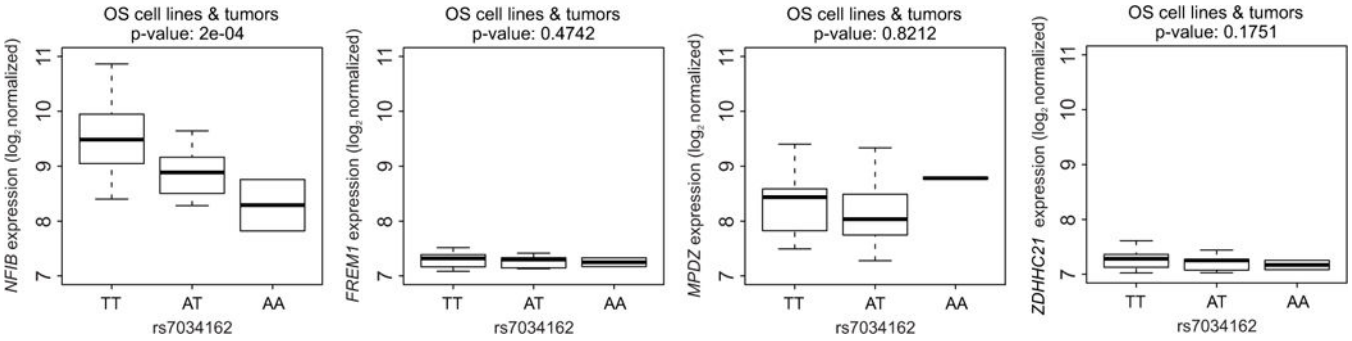

Figure 2. Relationship between the genotype of the metastasis-associated SNP, rs7034162, and expression of *NFIB* and other nearby protein-encoding genes *FREM1, ZDHHC1*, and *MPDZ* in osteosarcoma cell lines and tumors

Significance is based on linear regression comparing the distribution of *NFIB, FREM1, ZDHHC1*, and *MPDZ* expression between the TT homozygous non-risk genotype (N=34) of rs7034162 genotypes to the heterozygous risk AT (N=10) and the homozygous risk AA genotypes (N=2). These analyses were based on the publically available genotype and expression data from 17 osteosarcoma cell lines and 29 osteosarcoma tumors (20).

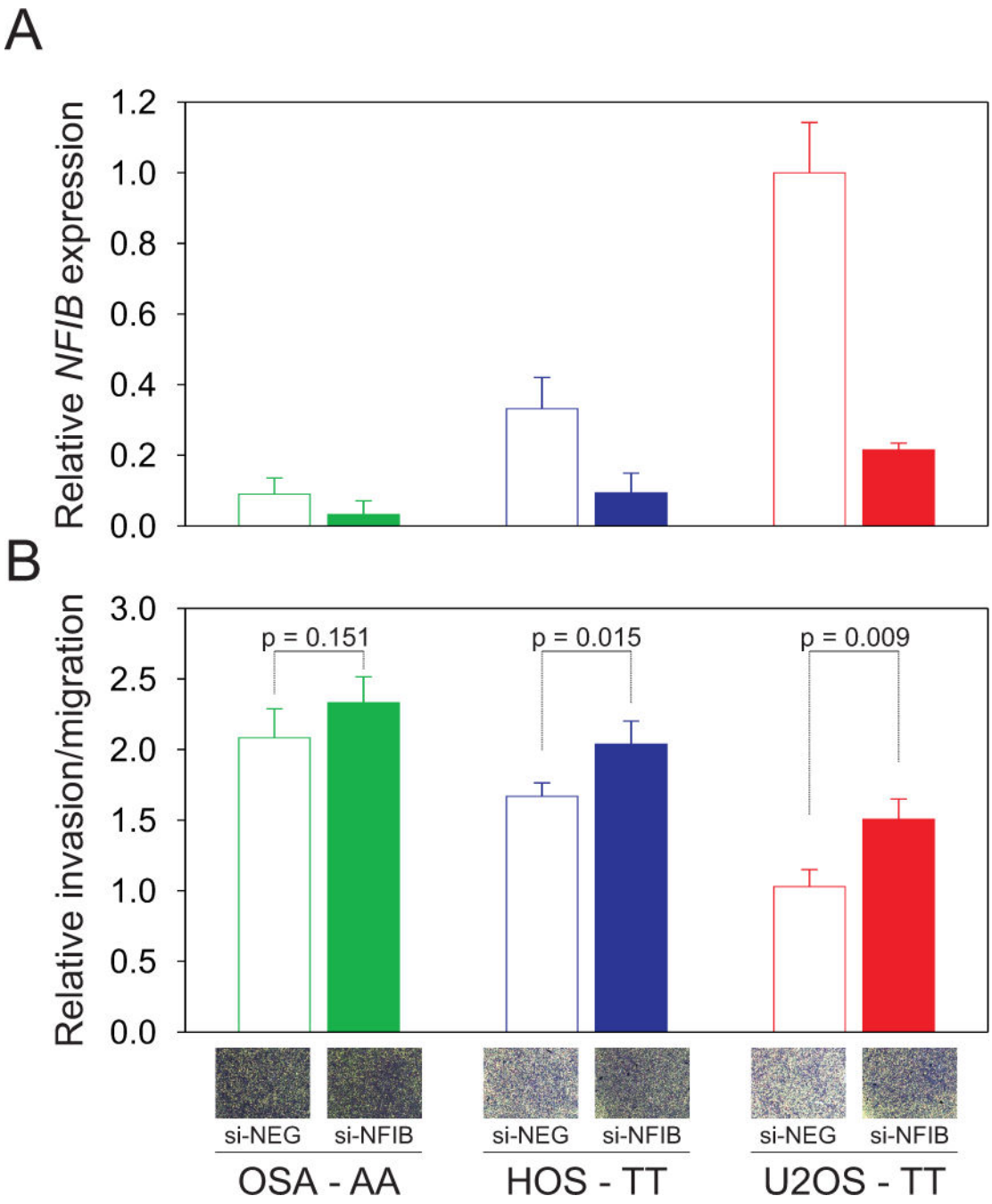

Figure 3. *NFIB* expression correlates with invasion and migration potential of human osteosarcoma cells

(**A**.) NFIB expression in OSA, HOS and U2OS cells was determined 48 hours after transfection with control siRNA (si-NEG) or siRNA targeting NFIB (si-NFIB). Graphs show relative expression compared with control treated U2OS cells. The rs7034162 genotype is shown for the osteosarcoma cell lines: U2OS and HOS cells carry the homozygous non-risk allele (TT), and OSA cells carry the homozygous risk allele (AA). (**B.**) 48 hours after NFIB suppression, cells were evaluated for migratory potential. Cells that invaded through the matrigel-coated membrane inserts were stained with crystal violet, air-

dried and bright field images were taken (inset photographs depict staining intensity differences). To quantify cell invasion/migration, the inserts were treated with 200μl of methanol and the absorbance measured in triplicate at 560 nm. Invading cells are depicted relative to control treated U2OS cell. Results of at least three experiments in triplicate are expressed as mean ± SD. The invasion and migration rate of each cell line was inversely correlated with *NFIB* expression levels.

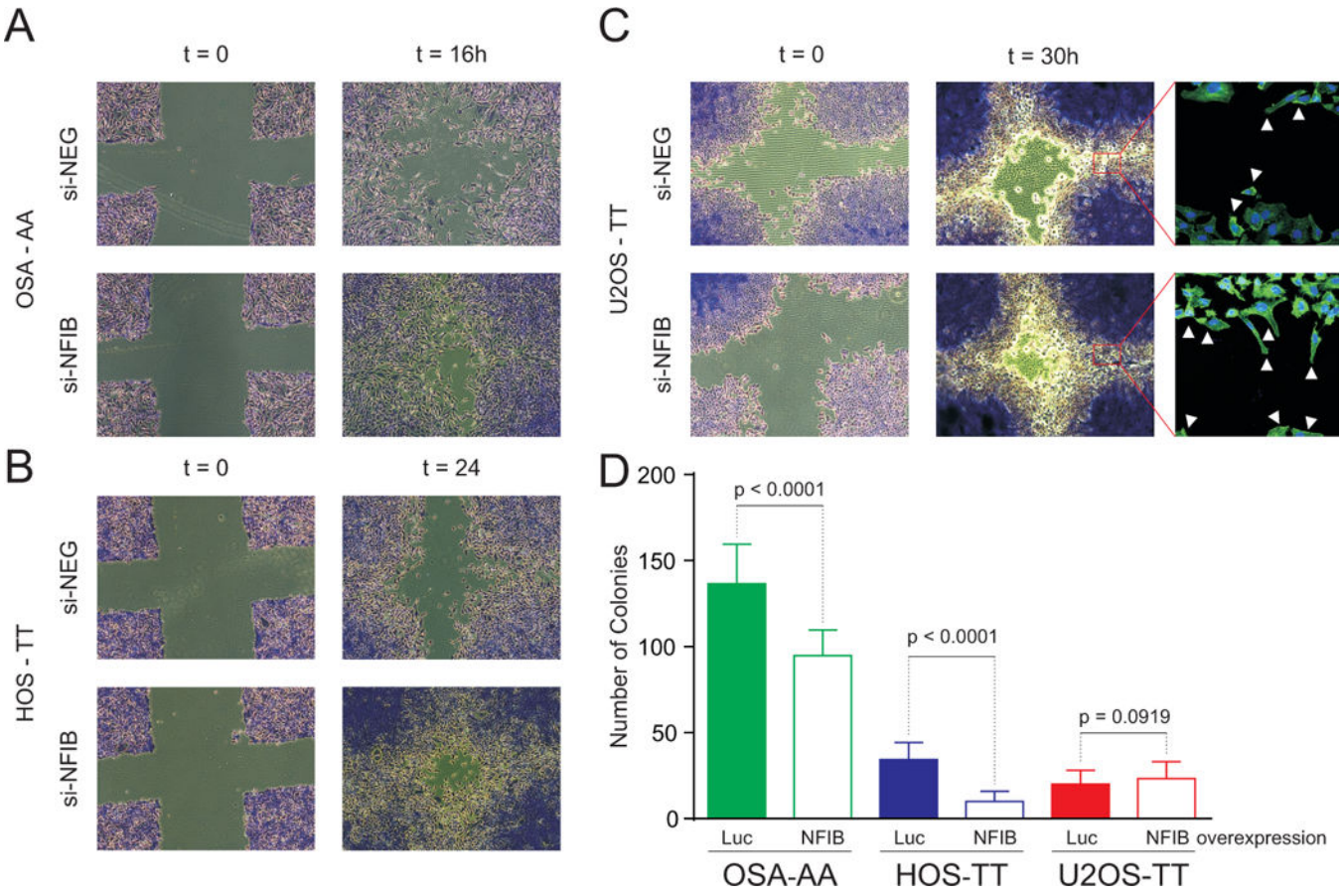

Figure 4. Increased migration and podia formation in NFIB suppressed human osteosarcoma cells

Subconfluent osteosarcoma cells were infected with the indicated siRNAs, and 48 hours post-infection wounds were made on the monolayers. Bright field images were taken at time 0 and 16, 24, and/or 30 hours (h). The wound healing cell migration and filamentous actin staining assays were done in triplicate for three cell lines: OSA (**A.**), HOS (**B.**) and U2OS (**C.**). The rs7034162 genotype is shown for the osteosarcoma cell lines: U2OS and HOS cells carry the homozygous non-risk allele (TT), and OSA cells carry the homozygous risk allele (AA). A representative example of the three independent experiments performed is shown. The cells showed increased migration after treatment with siRNA against NFIB (si-NFIB) compared with the si-NEG control, and the filamentous actin staining (far right) shows increased podia formation in the cells treated with si-NFIB. (**D.**) Soft agar colony formation assay in OSA, HOS, and U2OS cell lines. The HOS and OSA cells showed a significant reduction in colony formation after over-expressed of NFIB compared with the Luciferase (Luc) control.

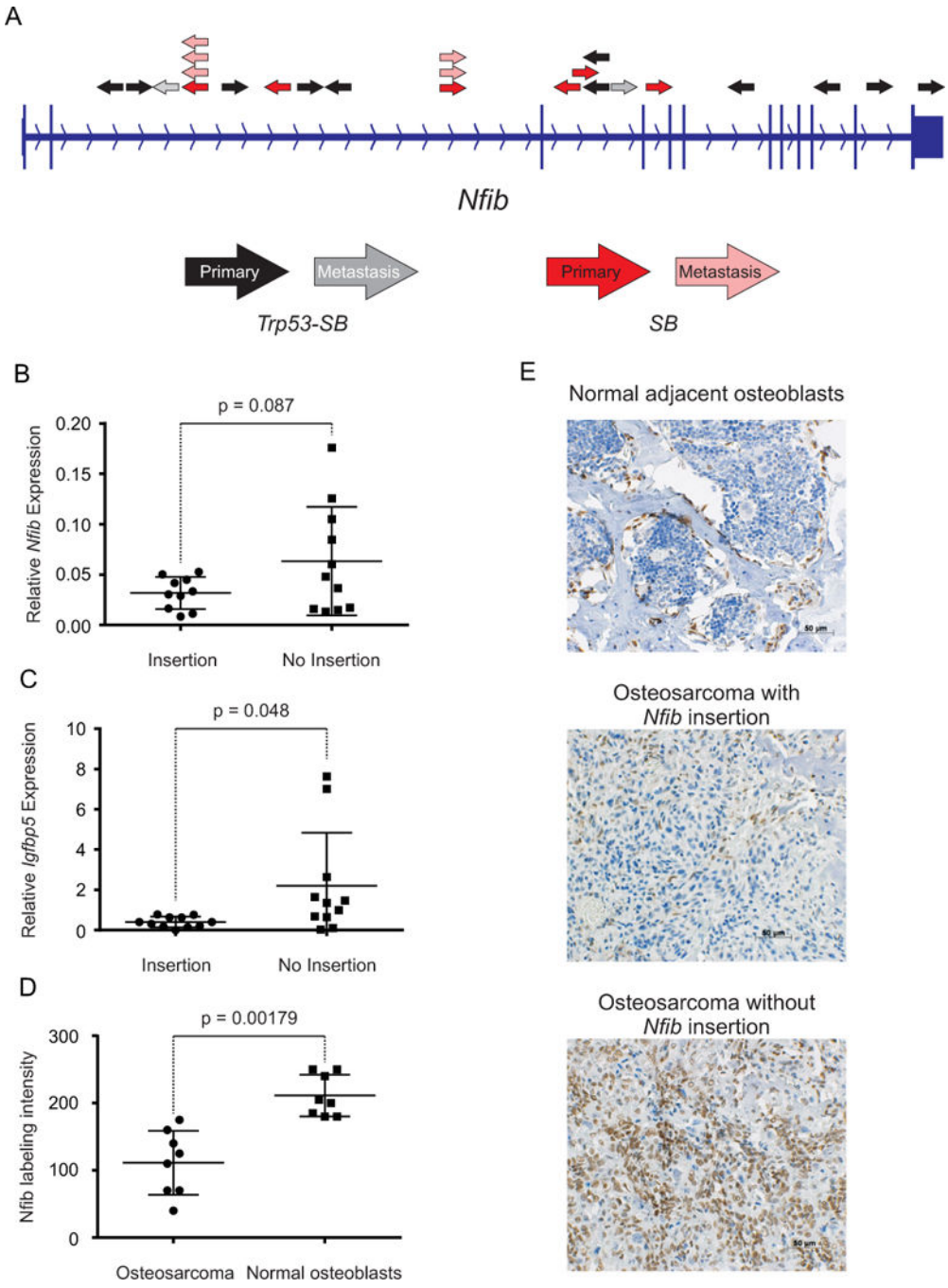

Figure 5. *Nfib* insertions from a *Sleeping Beauty* (SB) transposon screen for osteosarcoma in mice, and expression in mouse tumors

(**A.**) Diagram depicts T2/Onc insertion sites in *Nfib* from the SB transposon screen (23). Black and red arrows represent T2/Onc insertions identified in tumors from *Trp53-SB* and *SB* animals, respectively. Gray and light red arrows represent T2/Onc insertions identified in metastases from *Trp53-SB* and *SB* animals, respectively. The direction of the arrows represents the direction of the mouse stem cell virus (MSCV) LTR and splice donor (SD) sequence of T2/Onc. RT-PCR analysis of Nfib (**B.**) and Igfbp5 (**C.**) expression in tumors

with and without transposon insertions in *Nfib*. (**D.**) Semi-quantitative immunohistochemical scores for nuclear NFIB labeling in sections of mouse osteosarcomas with *Nfib* insertions and in normal adjacent osteoblasts. (**E.**) Immunohistochemical staining (brown) for NFIB in sections containing mouse osteosarcomas with or without an *Nfib* insertion and adjacent, normal osteoblasts to evaluate tissue-specific changes in NFIB expression. A two-tailed ttest was used to estimate the *P*-values for the differences in *Nfib* and/or *Igfbp5* expression.

Table 1

Summary of the top GWAS and imputed SNP associations with metastasis at diagnosis in the discovery and replication studies.

dbSNP locus	Chr: Position[a]	Allele[b]	Stage	Ancestry[c]	Cases with mets.		Cases without mets.		P value	OR (95% CI)
					Total	EAF	Total	EAF		
rs2890982	Chr9: 14181653	C/T	Discovery	EUR	122	0.25	419	0.11	4.36×10^{-7}	2.69 (1.83–3.94)
9p24.1			Replication 1	EUR	24	0.33	61	0.12	3.71×10^{-3}	3.38 (1.47–7.80)
			Replication 2	EUR	19	0.16	122	0.13	0.571	1.35 (0.47–3.87)
			Combined	EUR	165		602		4.98×10^{-8}	2.60 (1.87–3.62)
rs7034162	Chr9: 14190287	T/A	Discovery	EUR	122	0.25	419	0.11	1.37×10^{-7}	2.87 (1.94–4.24)
9p24.1			Replication 1	EUR	24	0.29	61	0.10	4.03×10^{-3}	3.14 (1.37–7.20)
			Replication 2	EUR	19	0.11	122	0.12	0.723	0.81 (0.25–2.62)
			Combined	EUR	165		602		3.29×10^{-8}	2.62 (1.86–3.68)
			Replication 3	AFR	22	0.43	39	0.25	0.061	2.08 (0.97–4.47)
			Replication 4	Brazil	40	0.21	67	0.12	0.078	1.97 (0.93–4.18)
			Combined	All	227		708		1.22×10^{-9}	2.43 (1.83–3.24)

Abbreviations: EAF, effect (coded) allele frequency; mets., metastasis at diagnosis; OR, odds ratio; CI, confidence interval.

EUR, European ancestry; AFR, African ancestry; Brazil, Brazilian ancestry.

[a] Build 36 position;

[b] Reference/Effect allele;

[c] Ancestry based on a STRUCTURE and principal component analysis.